Available online at www.sciencedirect.com

SciVerse ScienceDirect

Acta Materialia 60 (2012) 8–21

Acta MATERIALIA

www.elsevier.com/locate/actamat

Effects of particle arrangement and particle damage on the mechanical response of metal matrix nanocomposites: A numerical analysis

Elliot Law, Sze Dai Pang *, Ser Tong Quek

Department of Civil and Environmental Engineering, National University of Singapore, Block E1A, #07-03, 1 Engineering Drive 2, Singapore 117576, Singapore

Received 25 July 2011; received in revised form 21 September 2011; accepted 21 September 2011
Available online 28 October 2011

Abstract

The spatial distribution of reinforcement particles has a significant effect on the mechanical response and damage evolution of metal matrix composites (MMCs). It is observed that particle clustering leads to higher flow stress, earlier particle damage, as well as lower overall failure strain. In recent years, experimental studies have shown that reducing the size of particles to the nanoscale dramatically increases the mechanical strength of MMCs even at low particle volume fractions. However, the effects of particle distribution and particle damage on the mechanical response of these metal matrix nanocomposites, which may be different from that observed in normal MMCs, has not been widely explored. In this paper, these effects are investigated numerically using plane strain discrete dislocation simulations. The results show that non-clustered random and highly clustered particle arrangements result in the highest and lowest flow stress, respectively. The effect of particle fracture on the overall response of the nanocomposite is also more significant for non-clustered random and mildly clustered particle arrangements, in which particle damage begins earlier and the fraction of damaged particles is higher, compared to regular rectangular and highly clustered arrangements.

Keywords: Metal matrix composites (MMCs); Nanoparticles; Discrete dislocation dynamics; Plasticity; Particle clustering

1. Introduction

The spatial distribution of reinforcement particles has been known to have a significant effect on the mechanical properties and damage evolution of metal matrix composites (MMCs). Mishnaevsky [1] found that the flow stress and degree of hardening of the composite material is lowest for a highly graded particle arrangement but highest for a regular microstructure. Composites with clustered particles show higher flow stress due to more severely strain-hardened matrix compared with composites with uniformly distributed particles [2]. However, the overall failure strain is significantly lower for composites with clustered particles [3]. In addition, numerical computations show that the effective stresses and local stress and strain fields are much higher in microstructures with random particle distribution compared to a regular distribution. Nevertheless, particle arrangement does not influence the effective response of MMCs in the elastic and small plastic deformation regimes but is significant only at loads at which a significant number of particles begin to fail [1].

The effect of particle damage on the mechanical properties of MMCs has been discussed rather extensively in the literature [4–7]. Results from numerical simulations show that particle damage reduces the flow stress and degree of hardening considerably and the effect of particle damage is influenced by the spatial distribution of the reinforcement particles. Segurado et al. [8] reported that the fraction of damaged particles increases dramatically in a clustered particle arrangement compared to that of a uniform

* Corresponding author. Tel.: +65 6516 2799; fax: +65 6779 1635.
E-mail address: ceepsd@nus.edu.sg (S.D. Pang).

1359-6454/$36.00
doi:10.1016/j.actamat.2011.09.033

distribution due to higher average maximum principle stress and its standard deviation in composites with non-homogeneous particle distribution. In addition, Ayyar et al. [9] showed that MMCs with an ordered distribution of particles and uniform particle fracture strength have the highest strength to failure, but a uniform distribution of particles having fracture strength that follows a Weibull distribution results in the lowest strength to failure.

In recent years, many experimental results have shown that reducing the size of particles to the nanoscale dramatically improves the mechanical properties of MMCs such as tensile strength, hardness and creep resistance even at very low particle volume fractions while preserving good ductility [10–12]. This is due to the activation of strengthening mechanisms operating at the nanoscale within the metallic matrix such as Orowan strengthening [13,14]. However, the effects of particle arrangement and particle damage on the mechanical response of these metal matrix nanocomposites (MMNCs), which may be different from that observed in conventional MMCs due to the different dominant strengthening mechanisms in both types of material, have not been widely explored even though experimental studies have reported that agglomeration of nanoparticles (i.e. formation into coarse clusters) has detrimental effects on the mechanical properties of MMNCs.

In this paper, the effects of particle arrangement and particle damage on the mechanical response of MMNCs will be investigated numerically using discrete dislocation simulations. This is because the size effect must be considered for MMNCs as the size of the particles is at the nanoscale and distance between particles approaches the mean free path of dislocations [15]. It is well known that classical plasticity laws are unable to capture the size effect and are only useful at characteristic sizes greater than 10 μm where the effect of individual dislocation processes is insignificant and the material can be viewed as homogeneous. At the nanoscale, dislocations should be accounted for in a discrete manner. For a range of characteristic size between tens to hundreds of nanometers, the discrete dislocation approach is one of the most suitable methods for investigating the mechanical response of a plastic material due to the collective motion of dislocations [16,17].

2. Discrete dislocation formulation

The discrete dislocation plasticity framework used in this study follows closely the formulation developed by Van der Giessen and Needleman [18] which is outlined here; further details and references are given in Ref. [18] and their subsequent works [19–21]. The nanocomposite is considered as linear elastic isotropic body which contains elastic particles and has a distribution of dislocations in the matrix material. Plasticity originates from the motion of the edge dislocations, which are regarded as line defects in the matrix material. The current state of the body in terms of the displacement, strain and stress fields can be written as the superposition of two fields: the dislocation field and the image field. The dislocation field is associated with the dislocations in their current configuration but in an infinite medium of the homogeneous matrix material; the solution for the dislocation field can be obtained from literature [22]. The image field corrects for the actual boundary conditions and the presence of particles, and can be solved as a linear elastic boundary value problem using the finite-element method.

Constitutive relations are used to describe the nucleation, motion and annihilation of dislocations. Firstly, assuming dislocation glide only, the force f which acts on a dislocation with Burgers vector magnitude b and causes it to move with velocity v along its slip plane is directly proportional to the resolved shear stress τ_{rss} acting on the dislocation. This can be expressed as $f = \tau_{\mathrm{rss}} b = Bv$ where B is the drag coefficient. Furthermore, obstacles to dislocation motion modelled as fixed points on a slip plane are distributed randomly in the matrix to account for the effects of small precipitates or impurities and dislocations on other slip systems in blocking slip. A dislocation moving towards an obstacle or impurity will initially be pinned at the obstacle and can only bypass the obstacle when the resolved shear stress on the dislocation exceeds the strength of the obstacle or impurity τ_{obs}. Secondly, new dislocation pairs are generated by simulating Frank–Read sources: a point source located on a slip plane will generate a pair of opposite dislocations when the magnitude of the resolved shear stress at the source exceeds the nucleation strength τ_{nuc} during a period of time t_{nuc}. Thirdly, annihilation of two opposite dislocations occurs when they are within a material-dependent, critical annihilation distance $L_{\mathrm{e}} = 6b$ [18]. However, in the present study, dislocation motion on every slip plane will be tracked to determine whether annihilation of dislocation occurs; once a pair of opposite dislocations has crossed paths, they will be considered as annihilated. This tracking method allows for the use of greater time-steps in the discrete dislocation simulations.

The discrete dislocation formulation is implemented in a two-dimensional plane strain unit cell model with periodic boundary conditions shown in Fig. 1. The unit cell contains equally spaced horizontal slip planes with the spacing between slip planes $d = 100b$. Due to the periodicity of the unit cell, dislocations exiting the unit cell through one side will re-enter through the opposite side. Simple shear deformation is applied on the unit cell through prescribed displacements along the top and bottom edges and the overall shear stress–strain response is computed. The overall or average shear stress τ_{ave} and average shear strain γ_{ave} of the nanocomposite are calculated, respectively, from the traction and displacement along the top and bottom edges of the unit cell. Computation of the deformation history, assuming small strain kinematics, is carried out in an incremental manner.

The numerical results presented in this study are obtained using representative elastic properties for aluminum matrix and silicon carbide reinforcement nanoparticles; these material properties and various

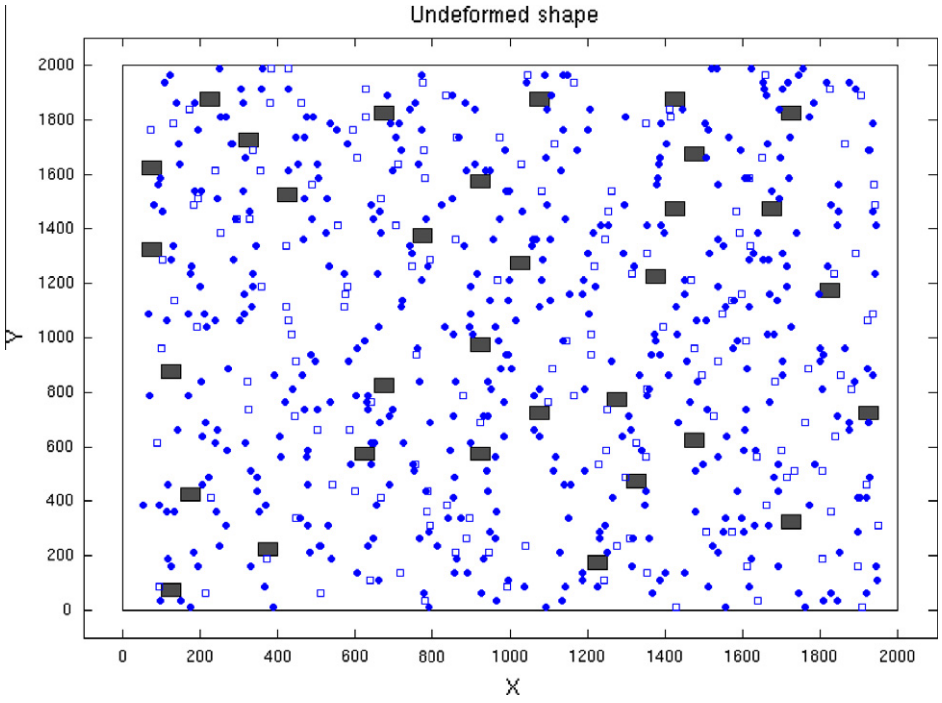

Fig. 1. Two-dimensional unit cell model showing the locations of the particles (shaded boxes), dislocation sources (white rectangular markers) and impurities represented by point obstacles (black circular spots).

parameters used to describe dislocation processes in the constitutive relations follow that in Law et al. [23]. For regular particle arrangements, the mean overall response is computed using at least three different realizations of random dislocation source and impurity distributions; for irregular particle arrangements, at least 12 different realizations of dislocation source, impurity and particle distributions are used. As shown in Ref. [23], the overall response is highly dependent on the distribution of these features.

3. Effect of particle arrangement in MMNCs with undamaged particles

Fig. 2 shows the mean overall response of the composite material with 2% particle volume fraction and uniform particle size of 25 nm for different regular particle arrangements, while Fig. 3 shows the corresponding distributions of particles and dislocations within the matrix. A regular rectangular arrangement of particles results in the lowest flow stress and degree of hardening as the number of slip planes blocked by the particles is minimized. On the other hand, the mean overall response for diagonal arrangements depends on the w/h ratio as shown in Fig. 2: increasing w/h ratio results in higher flow stress. This is because number of slip planes blocked by the particles increases with the w/h ratio as the width of the unreinforced (horizontal) bands in the matrix decreases as shown in Fig. 3b–d. Therefore, more dislocations are impeded by the particles if the regular arrangement of particles results in many blocked slip planes, which results in improved flow stress and degree of hardening.

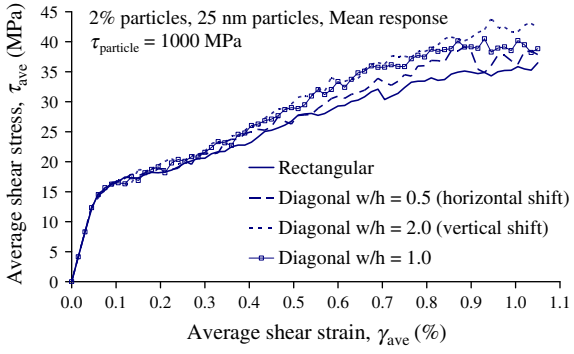

Fig. 2. Mean overall response of composite material with undamaged particles for different regular particle arrangements (w and h are the distance between the diagonal lines of particles in the x and y-directions, respectively).

Non-clustered random particle arrangements are created using the random sequential adsorption (RSA) algorithm [24] in which the particle centre positions are generated randomly and sequentially: the distances between particle i and all the particles previously accepted $j = 1, 2, \ldots, i-1$ have to exceed a minimum value s imposed by practical limitations to prevent overlap of particles with each other as well as the boundaries of the unit cell. Clustered particle arrangements are generated following Mishnaevsky et al. [3], in which the coordinates of particle centres in a cluster are calculated as follows: the distance between cluster centre and particle centre follows a Gauss distribution, while the angle between the horizontal line and the line between the centre of cluster and particle follows a uniform random distribution. The clusters are randomly distributed within the matrix. The standard deviations of the distribution of

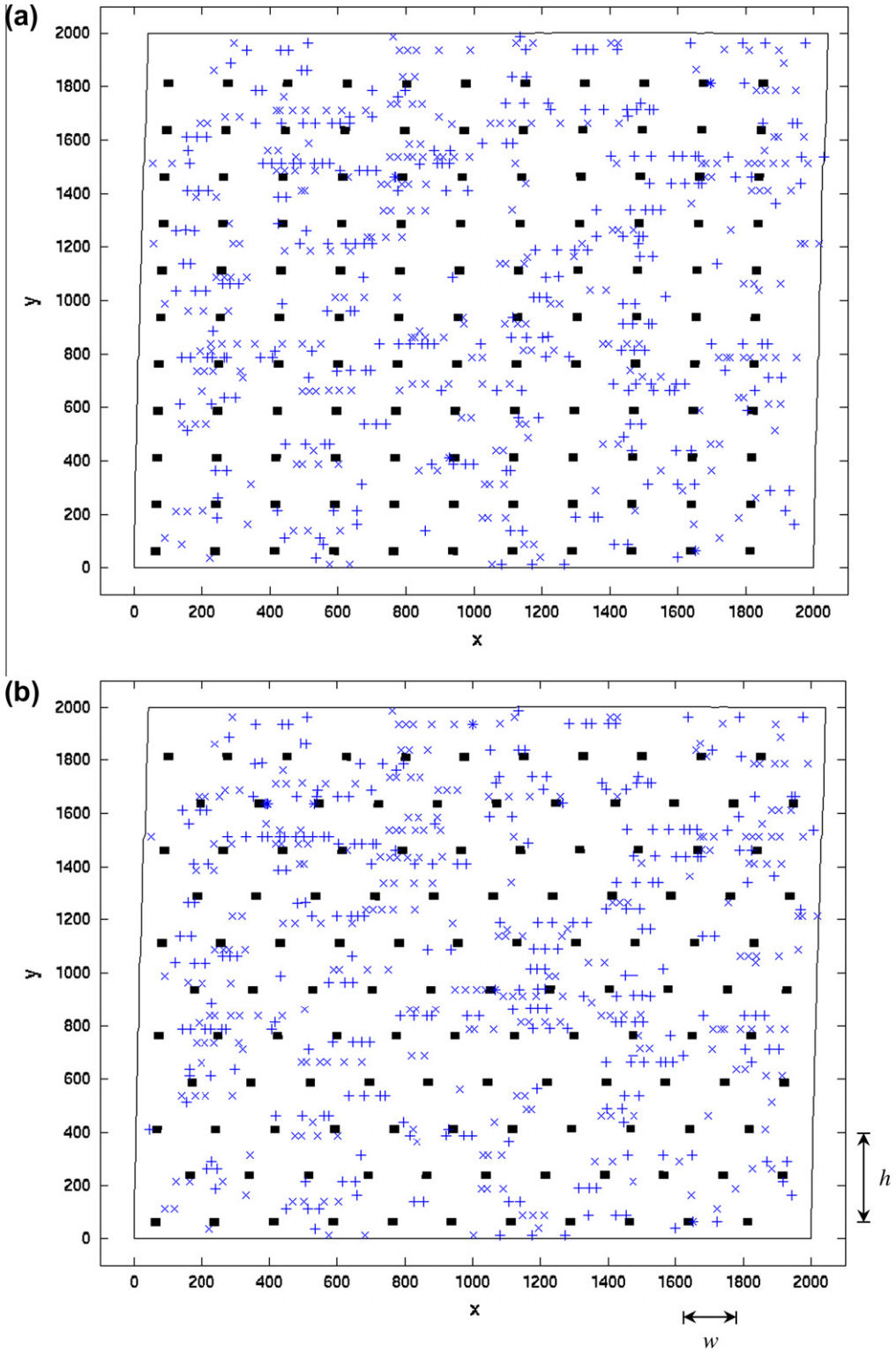

Fig. 3. Distribution of dislocations (denoted by "+" and "×") and particles (shaded boxes) at $\gamma_{ave} = 1.05\%$ for (a) rectangular, (b) diagonal $w/h = 0.5$, (c) diagonal $w/h = 2.0$, and (d) diagonal $w/h = 1.0$ particle arrangements.

particle coordinates in a cluster can be varied to produce different degrees of clustering. Segurado et al. [8], Rintoul and Torquato [24], and Segurado and Llorca [25], among others, have also discussed other methods for generating clustered microstructures such as the modified random sequential adsorption process (MRSA) which may produce better reconstructions of actual particle distributions observed in composite materials. However, these methods are particularly useful for composite materials with large particle volume fractions; for particle volume fractions <20%, the

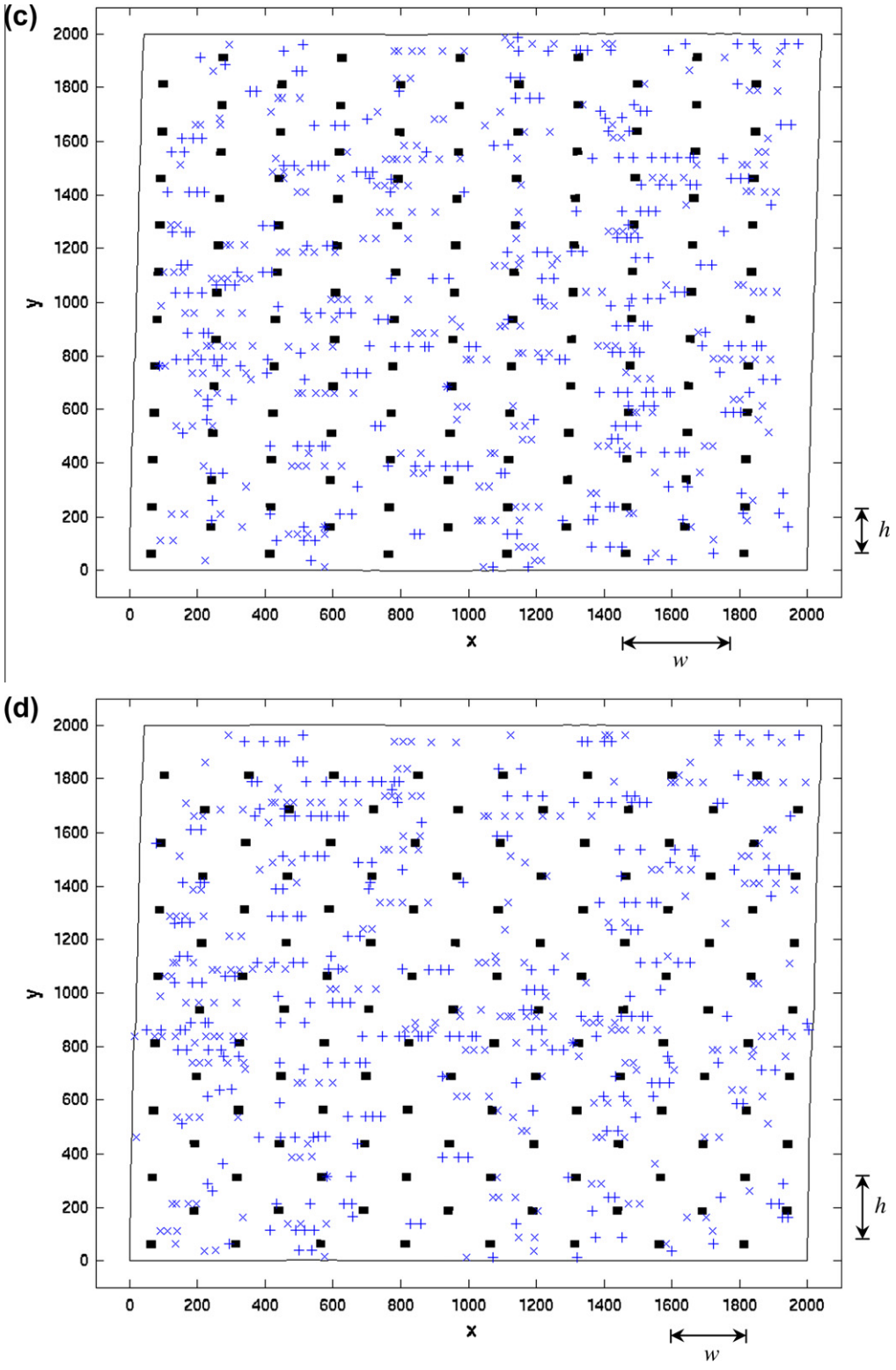

Fig 3. *(continued)*

RSA algorithm is able to produce satisfactorily representative particle distributions compared to the more advanced techniques.

The degree of particle clustering can be described quantitatively using several measures such as the average nearest-neighbour distance (NND), the nearest-neighbour index (NNI, i.e. the ratio of observed to expected NND in which the expected NND for two-dimensional space is the square root of the total area of the unit cell divided by the square root of the total number of particles), the

coefficient of variation of the mean near-neighbour distance (COV_d) and the radial distribution function. The first three mainly provide information about the particle arrangement within individual clusters, while the radial distribution function also includes data on the interaction among the clusters [8]. Nevertheless, the NND, NNI and COV_d are more convenient measures as a single value is used to describe the particle distribution; also, at low particle volume fractions the interaction between clusters is not expected to be significant. The NNI shall be used here to quantify the degree of particle clustering in which a smaller NNI value represents a higher degree of clustering.

Fig. 4 shows the mean overall response of the composite material with 2% particle volume fraction and a uniform particle size of 25 nm for different irregular particle arrangements. A regular rectangular particle arrangement gives the lowest flow stress and degree of hardening, while a non-clustered random arrangement results in the highest flow stress and degree of hardening. This is because the number of slip planes blocked by the particles is minimized for the rectangular arrangement and there are many large veins of unreinforced matrix as shown in Fig. 3a. Dislocations can move relatively easily with little hindrance on the many unobstructed slip planes. On the other hand, most slip planes are blocked by particles when the arrangement is random as shown in Fig. 5a. Dislocations unable to bypass the particles will form many dislocation pile-ups, which retard the generation of new dislocations and hinder the motion of existing dislocations. Impediment to dislocation motion increases the flow stress and degree of hardening of the metallic nanocomposite.

Fig. 4 also shows that a high degree of particle clustering results in lower flow stress and degree of hardening with increasing applied deformation, compared to the cases with mild and moderate degrees of clustering. As shown in Fig. 5b–d, higher degrees of clustering results in more unreinforced regions and unobstructed slip planes in the matrix; there is minimal hindrance to the motion of dislocations. This effect is more significant with increasing applied deformation when localization of dislocation activity begins to occur on the unobstructed slip planes. A mild degree of particle clustering, however, does not result in any appreciable change in the mean overall response compared to the non-clustered random particle arrangement. This is because the particles are still able to effectively block the motion of dislocations on most slip planes.

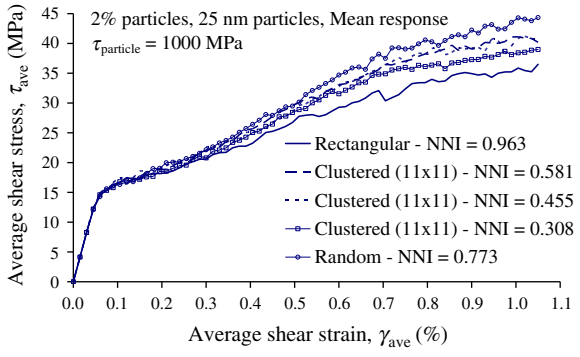

Fig. 4. Mean overall response of composite material with undamaged particles for different irregular particle arrangements.

Therefore, for composite materials with undamaged nanoparticles the flow stress and degree of hardening is lowest for regular rectangular and highly clustered particle arrangements in which there are many unimpeded slip planes on which dislocations can move with minimal obstruction. On the other hand, non-clustered random and mildly clustered arrangements of particles result in improved mean overall response compared to a regular rectangular arrangement due to the increased resistance to dislocation motion.

4. Effect of particle damage on mechanical response of MMNCs

In the simulations, a particle is considered fully damaged when the average maximum principal stress within the particle reaches or exceeds its fracture strength. Since the stress distribution is not uniform within each particle, the average stresses for every particle are computed based on several sampling points. The particle fracture strength $\tau_{particle}$ can either be uniform or follows a certain distribution. There is ample evidence that the strength of brittle ceramic particles follows the Weibull distribution [8,9,27]. However, for simplicity, uniform particle fracture strength is adopted for the simulations presented here. Moreover, damaged particles are not removed from the unit cell as they may still contribute to stiffening or strengthening [26]. Instead, dislocations will be allowed to glide past the damaged particles.

4.1. Effects of particle fracture strength, particle volume fraction and particle size

Fig. 6 shows the mean overall response of the composite material with a non-clustered particle arrangement, a 2% particle volume fraction and a particle size of 50 nm. When particle damage occurs easily, large dislocation pile-ups are unable to form against the particles. Dislocations released by a damaged particle will also pile up against another particle, which will quickly lead to the damage of this particle. Hence, the flow stress decreases with decreasing particle fracture strength because of the reduced resistance to the motion of dislocations. On the other hand, when the particle fracture strength is high, the particles can impede the motion of dislocation effectively and allow for larger dislocation pile-ups to be formed since the particles are more tolerant to damage. Fig. 6 also shows that the effect of particle damage is significant at very low particle fracture strength. The flow stress at applied shear strain $\gamma_{ave} = 1.0\%$ for the case with particle fracture strength of 100 MPa is approximately 10% lower compared to the case with no particle damage. However, there is little difference between the case with particle fracture strength of 200 MPa, in

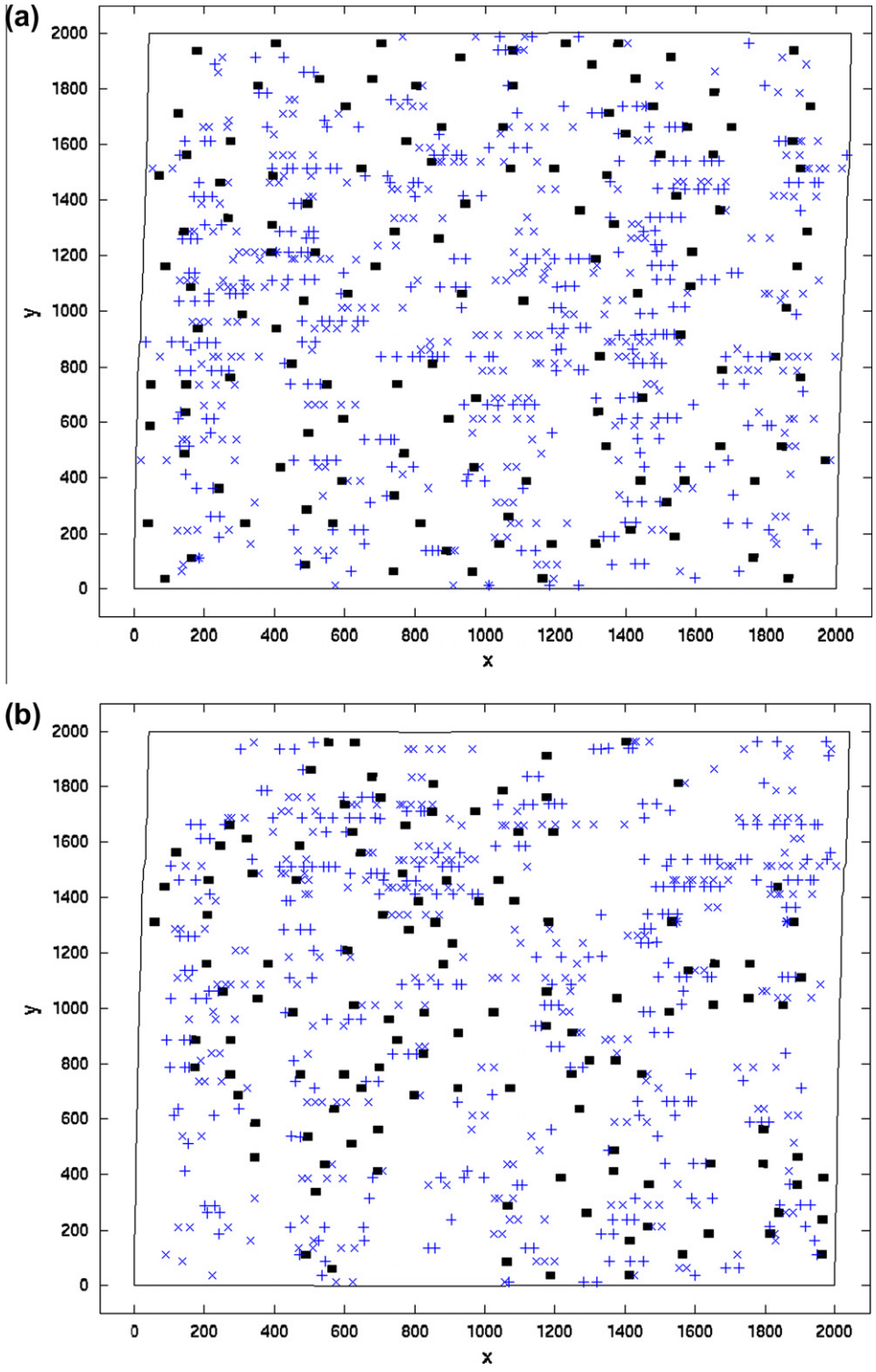

Fig. 5. Distribution of dislocations and particles at $\gamma_{ave} = 1.05\%$ for (a) non-clustered random, (b) mildly clustered (NNI = 0.581), (c) moderately clustered (NNI = 0.455), and (d) highly clustered (NNI = 0.308) particle arrangements.

which the fraction of damaged particles is only 5% at applied shear strain $\gamma_{ave} = 1.0\%$, and that with particle fracture strength of 1000 MPa in which particle damage does not occur. Hence, the effect of particle damage on the mean overall response of the composite material is only significant when the fraction of damaged particles is relatively high.

Fig. 7 shows the mean overall response of the composite material with a random particle arrangement, a 5% particle volume fraction and a particle size of 50 nm. The trends

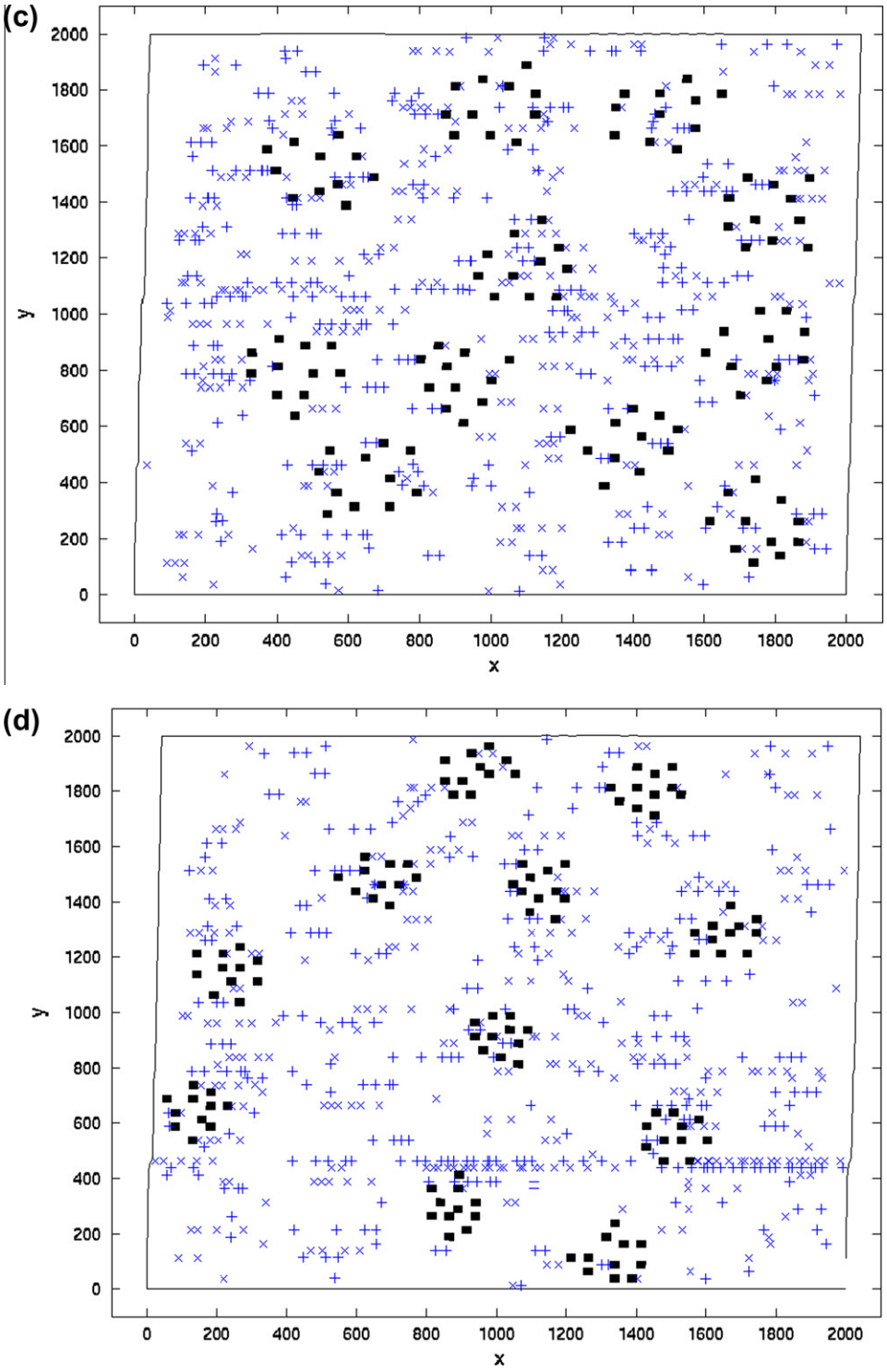

Fig 5. *(continued)*

shown are similar to those discussed previously for the case of 2% particle volume fraction as shown earlier in Fig. 6. However, the effect of particle failure seems to be slightly more significant with increased particle volume fraction. Fig. 6a shows that the flow stress at applied shear strain $\gamma_{ave} = 1.0\%$ for the cases with particle fracture strengths of 100 and 200 MPa is approximately 40% and 10% lower, respectively, compared to the case with no particle damage (in which the particle fracture strength is 1000 MPa). Moreover, the fraction of damaged particles is higher with increased particle volume fraction as shown in Fig. 7b for the case of 5% particle volume fraction compared to Fig. 6b for the case of 2% particle volume fraction. This is because there are more dislocation pile-ups and greater load transfer from the matrix to the relatively stronger reinforcement particles with increasing particle volume frac-

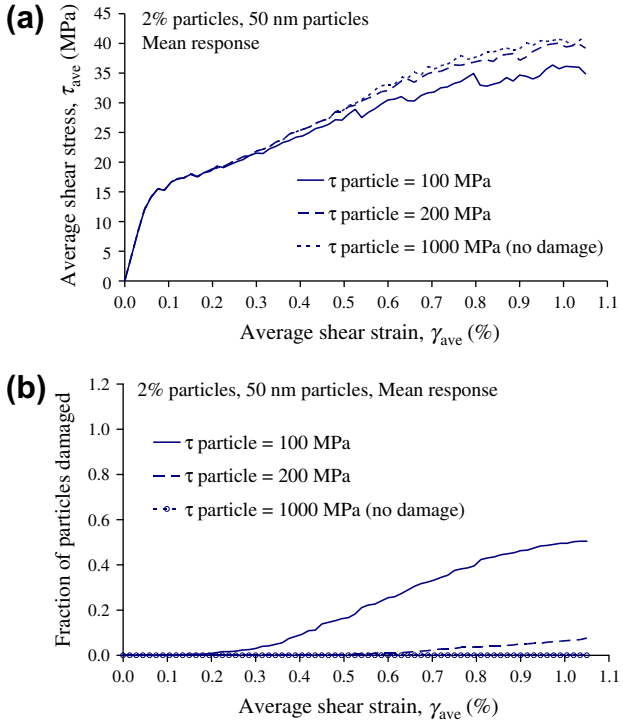

Fig. 6. (a) Mean overall response of composite material with different particle fracture strength, and (b) the corresponding fraction of damaged particles for random particle distributions with 2% particle volume fraction and a particle size of 50 nm.

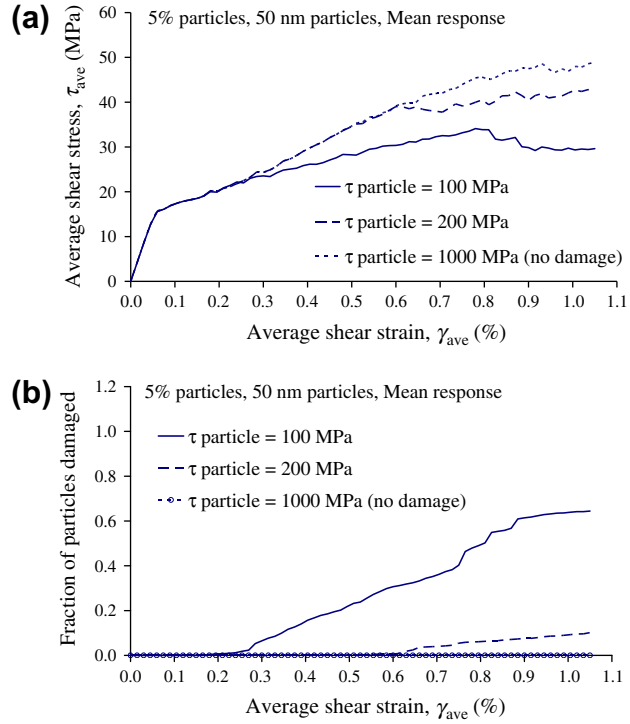

Fig. 7. (a) Mean overall response of composite material with different particle fracture strengths, and (b) the corresponding fraction of damaged particles for random particle distributions with 5% particle volume fraction and a particle size of 50 nm.

tion. Consequently, the average stresses in the reinforcement phase increases with greater particle volume fraction which results in a higher probability of particle damage.

Figs. 8 and 9 show the mean overall response for a composite material with a 2% particle volume fraction and particle sizes of 100 and 25 nm, respectively. The flow stress at applied shear strain $\gamma_{ave} = 1.0\%$ for the case with a particle fracture strength of 100 MPa is approximately 10% and is 35% lower compared to the case with no particle damage, for particle sizes of 100 and 25 nm, respectively. At the same particle volume fraction, the number of particles increases with decreasing particle size; as reported in Ref. [23] and in numerous experimental studies, the increased number of particles caused by reducing the particle size results in a greater impediment to dislocation motion and hence increased strength of the metallic nanocomposite. In addition, the greater number of particles leads to the formation of more dislocation pile-ups against the particles. These dislocation pile-ups are well distributed within the matrix and it is harder to find a weak region where dislocations can move relatively easily. Therefore, the average stress in the particles may be higher in the case with smaller particles because of the increased number of dislocation pile-ups. Moreover, dislocation pile-ups are formed quickly for the case with smaller particles since the mean free path of dislocations is smaller. Consequently, the onset of particle damage occurs earlier and the fraction of damaged particles increases with decreasing particle size as shown in Figs. 6b, 8b and 9b. Furthermore, the effect of particle damage is more significant because extensive particle damage is required to create a weak zone in the material. Conversely, when there are only a few large particles, fewer dislocation pile-ups are formed against the particles and it is easier for localization of dislocation activity to occur due to the presence of large unreinforced regions. Thus, the creation of new weak zones due to particle failure is not as critical as there are already significant unreinforced regions in the matrix for the case with large particles.

In conclusion, lower particle fracture strength results in lower composite flow stress, earlier onset of particle damage and a higher fraction of damaged particles. The effect of particle failure is more prominent with increasing particle volume fraction as there are more dislocation pile-ups, and load transfer from the matrix to the relatively stronger reinforcement particles becomes more significant. The effect of particle failure is also more pronounced with decreasing particle size assuming that particle fracture strength is independent of particle size, as there are more dislocation pile-ups in the metallic matrix and the average stresses in the particles are higher.

Nevertheless, the observations above are only valid if the particle fracture strength is independent of particle size. In actual fact, the fracture strength of ceramic particles increases with decreasing particle size due to the reduced probability of flaws that cause cracking and premature

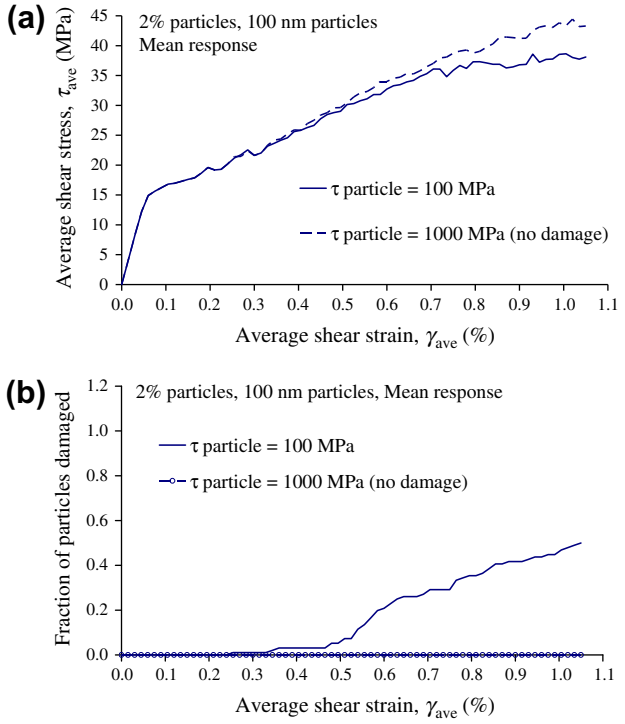

Fig. 8. (a) Mean overall response of composite material with different particle fracture strengths, and (b) the corresponding fraction of damaged particles for random particle distributions with 2% particle volume fraction and a particle size of 100 nm.

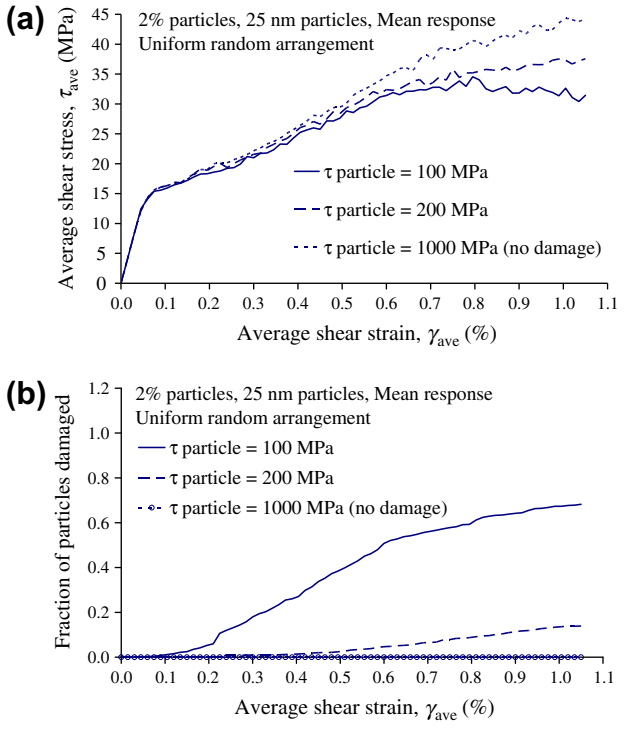

Fig. 9. (a) Mean overall response of composite material with different particle fracture strengths, and (b) the corresponding fraction of damaged particles for random particle distributions with 2% particle volume fraction and a particle size of 25 nm.

failure [14]. Hence, the effect of particle damage might not be more significant with decreasing particle size depending on the rate at which particle fracture strength increases with decreasing particle size.

4.2. Effect of particle arrangement

As shown in the previous section, the spatial distribution of reinforcement particles has a significant effect on the mean overall response of MMNCs with undamaged particles. Particle arrangement also affects the damage of particles in the nanocomposite.

Fig. 10 shows the mean overall response for a composite material with different particle fracture strengths and arrangements of particle. For a regular rectangular arrangement of particles, the effect of particle damage on the mean overall response is insignificant as it does not

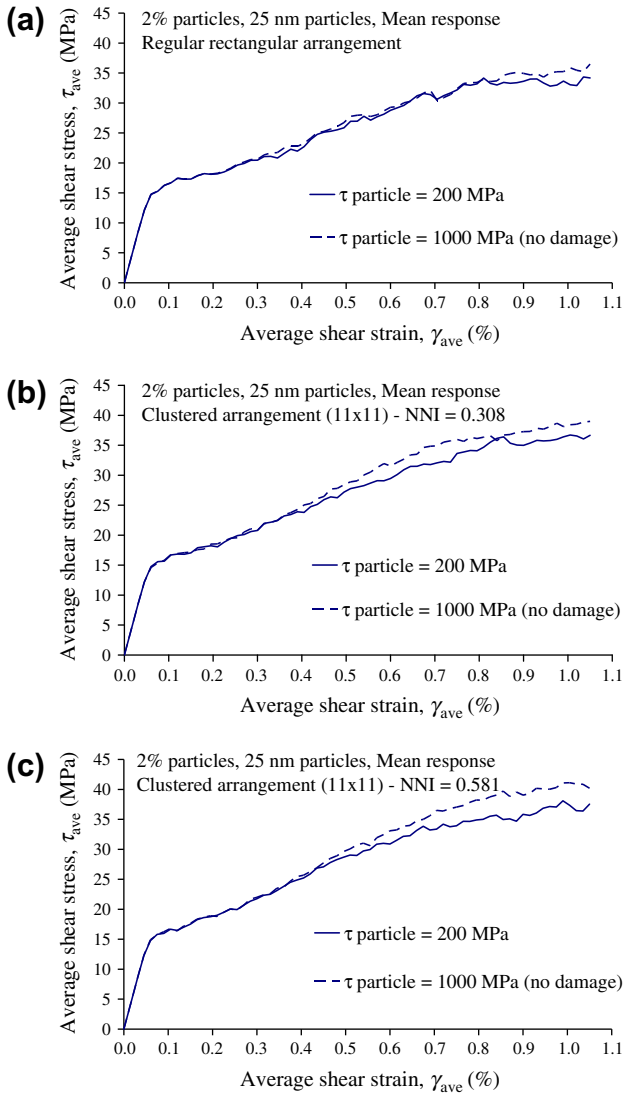

Fig. 10. Mean overall response of composite material with different particle fracture strengths for (a) regular rectangular, (b) highly clustered (NNI = 0.308) and (c) mildly clustered (NNI = 0.581) particle arrangements.

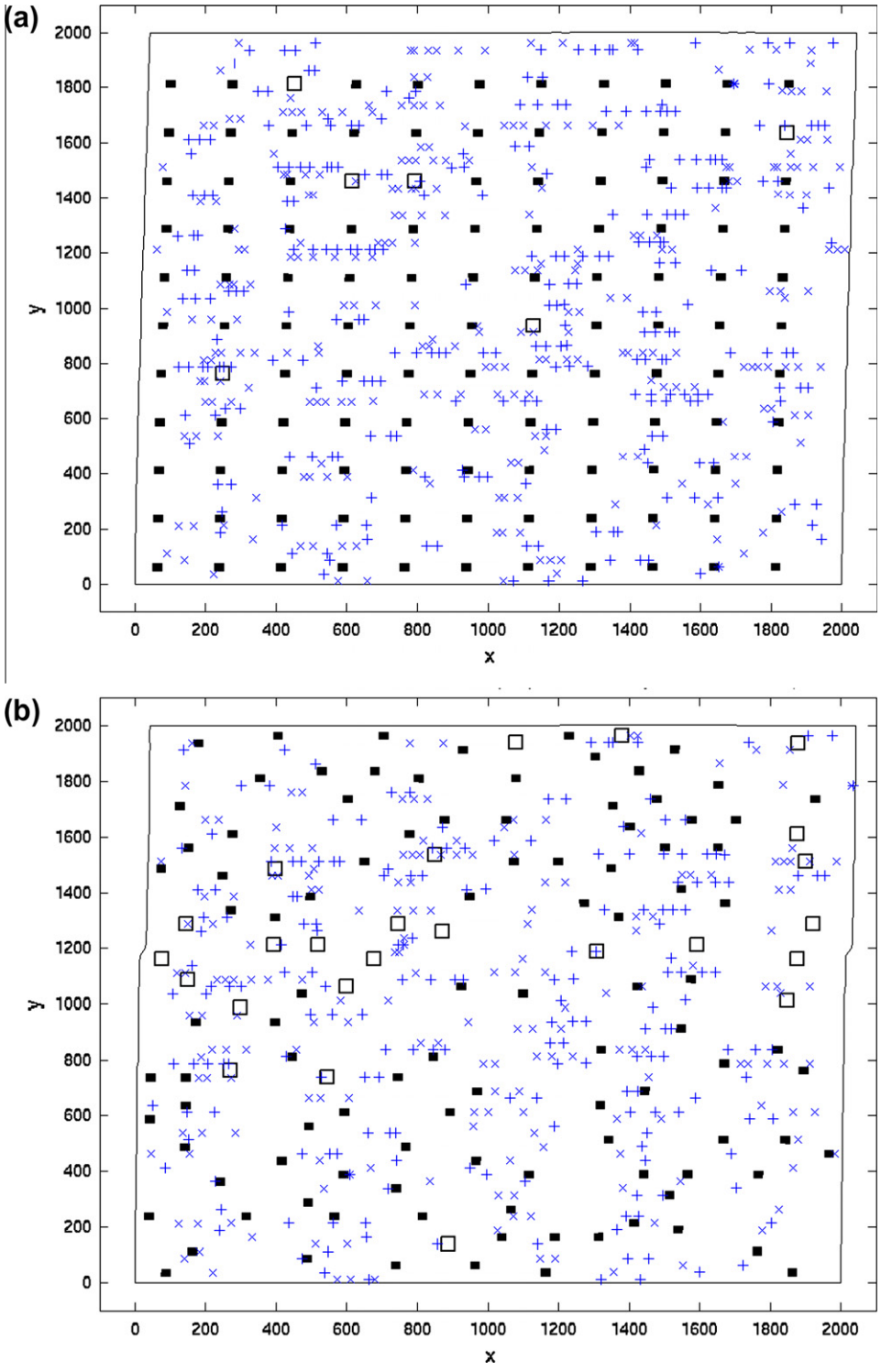

Fig. 11. Distribution of dislocations and particles at $\gamma_{ave} = 1.05\%$ for (a) regular rectangular, (b) non-clustered random, (c) mildly clustered (NNI = 0.581) and (d) highly clustered (NNI = 0.308) particle arrangements. Intact particles are denoted by shaded boxes, and damaged particles are represented by blanks; the fracture strength of the particles is 200 MPa.

result in substantial changes to the sequence of dislocation processes and the final distribution of dislocations as shown in Figs. 3a and 11a. This is because few dislocations are impeded by the particles. The same trend is observed for a composite material within a highly clustered particle arrangement, in which particle damage results in only a minor reduction in the flow stress and degree of hardening. On the other hand, the effect of particle damage on the mean overall response of the composite material is more significant for non-clustered random and mildly clustered particle arrangements. As these particle arrangements are more effective in blocking the motion of dislocations, many

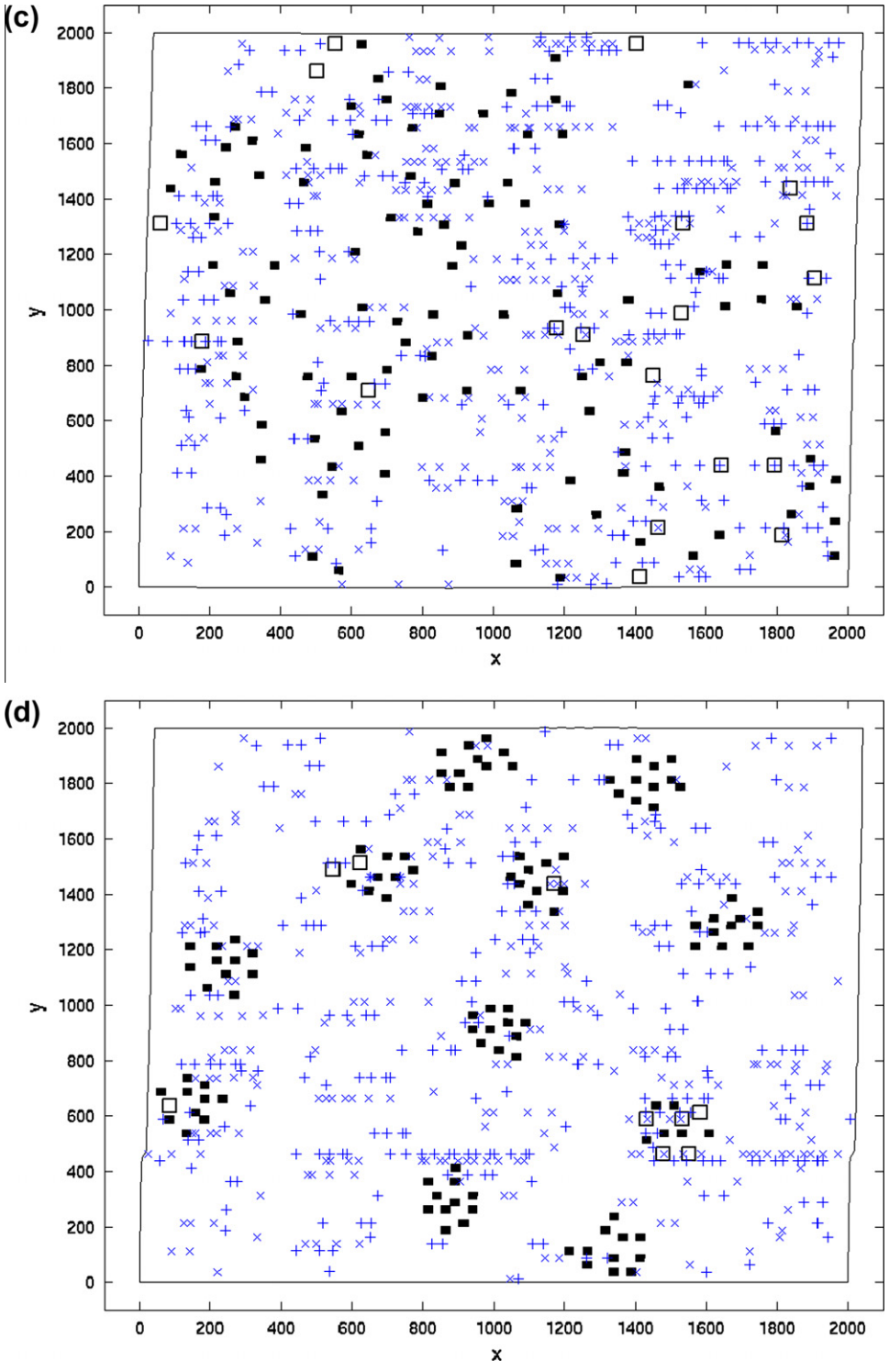

Fig 11. *(continued)*

impeded dislocations are suddenly released upon particle failure. Hence, particle damage results in fewer dislocation pile-ups in the matrix, which is evident when comparing Fig. 5a with Fig. 11b. This leads to lower flow stress and degree of hardening when particle failure occurs. Fig. 10b and c show that the flow stress at applied shear strain $\gamma_{ave} = 1.0\%$ for the case with a particle fracture strength of 200 MPa is approximately 5% and 15% lower, respectively, compared to the case with no particle damage (in which the fracture strength is 1000 MPa) for highly clustered and mildly clustered particle arrangements.

Due to the increased efficiency in impeding the motion of dislocations, the average stresses within the particles in non-clustered random and mildly clustered particle

arrangements are also higher compared to that in regular rectangular and highly clustered arrangements. Consequently, the fraction of damaged particles is also higher in the former cases as shown in Fig. 12. A greater fraction of particle damage must be achieved in these cases before the weakest path for localization of dislocation activity can be found compared to rectangular and highly clustered particle arrangements. Also, as shown in Fig. 11d, not all particles in a cluster will be damaged. The outermost particles will tend to fail first because they are under higher stresses due to the pile up of dislocations, whereas inner particles will be damaged later after the dislocations have bypassed the damaged periphery particles and begin to pile up against the inner particles.

Therefore, the damage of particles has a significant influence on the mean overall response of the composite material only when the particle arrangement results in effective obstruction of dislocation motion prior to particle failure. It is shown that non-clustered random and mildly clustered particle arrangements result in more particle damage compared to regular rectangular and highly clustered arrangements. This is in contrast with the behaviour reported for conventional MMCs in which the flow stress (for cases with undamaged particles) and fraction of damaged particles (for cases with damageable particles) increase with degree of clustering [8]. The reason for this difference is the different dominant strengthening mechanism in metallic nanocomposites compared to conventional MMCs; obstruction of dislocation motion is the principal mode of strengthening in metallic nanocomposites, whereas load transfer from matrix to the particles (i.e. constraint on deformation of the matrix surrounding the particles) governs strengthening in conventional MMCs.

The above results, which were obtained using discrete dislocation simulations, give a new insight into the mechanisms of the reinforcement in MMCs with nanosized particles. While it may be useful to compare these results with those obtained using other numerical modelling approaches such as size-dependent non-local plasticity formulations, such simulations have not been commonly adopted for MMCs. Nevertheless, results from the few such studies published in literature seem to suggest that non-local plasticity formulations can also be used to capture the size effects observed in MMCs and gives results comparable to those obtained with discrete dislocation approaches [28–31]. Furthermore, it would be extremely useful to compare and validate the numerical results obtained in this study with some benchmark experiments. However, at this point in time, such experimental work on metallic nanocomposites is rare. Consequently, these are potential areas of future research which should be further explored.

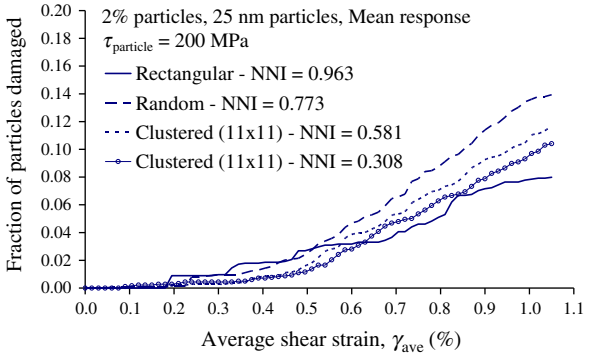

Fig. 12. Fraction of damaged particles for different particle arrangements with 2% particle volume fraction, a particle size of 25 nm, and $\tau_{particle} = 200$ MPa.

5. Conclusion

The flow stress for metallic nanocomposites with undamaged particles is lowest for rectangular and highly clustered particle arrangements, while non-clustered random and mildly clustered arrangements result in higher flow stress due to the greater impediment to dislocation motion. The effect of particle damage on the overall response of the nanocomposite is also more significant for non-clustered random and mildly clustered particle arrangements, in which particle damage begins earlier and the fraction of damaged particles is higher, compared to rectangular and highly clustered arrangements. Also, the effect of particle failure is more prominent with increasing particle volume fraction and decreasing particle size. This is because the increased efficiency in impeding the motion of dislocations results in higher average stresses within the particles.

References

[1] Mishnaevsky Jr LL. Acta Mater 2004;52:4177.
[2] Borbély A, Biermann H, Hartman O. Mater Sci Eng A 2001;313:34.
[3] Mishnaevsky Jr L, Derrien K, Baptiste D. Compos Sci Technol 2004;64:1805.
[4] Yang J, Cady C, Hu MS, Zok F, Mehrabian R, Evans AG. Acta Metall Mater 1990;38:2613.
[5] Finot M, Shen YL, Needleman A, Suresh S. Metall Mater Trans A 1994;25A:2403.
[6] Llorca J, González C. J Mech Phys Solids 1998;46:1.
[7] Sun LZ, Liu HT, Ju JW. Int J Numer Meth Eng 2003;56:2183.
[8] Segurado J, González C, Llorca J. Acta Mater 2003;51:2355.
[9] Ayyar A, Crawford GA, Williams JJ, Chawla N. Comp Mater Sci 2008;44:496.
[10] Ma ZY, Li YL, Liang Y, Zheng F, Bi J, Tjong SC. Mater Sci Eng A 1996;219:229.
[11] Cao G, Konishi H, Li XC. J Manuf Sci Eng 2008;130:031105.
[12] Mazahery A, Abdizadeh H, Baharvandi HR. Mater Sci Eng A 2009;518:61.
[13] Kang YC, Chan SLI. Mater Chem Phys 2004;85:438.
[14] Tjong SC. Adv Eng Mater 2007;9:639.
[15] Groh S, Devincre B, Kubin LP, Roos A, Feyel F, Chaboche JL. Mater Sci Eng A 2005;400–401:279.
[16] Bulatov VV, Cai W. Computer simulations of dislocations. Oxford: Oxford University Press; 2006.
[17] Neddleman A, Van der Giessen E. Mater Sci Eng A 2001;309–310:1.
[18] Van der Giessen E, Neddleman A. Modell Simul Mater Sci Eng 1995;3:689.

[19] Balint DS, Deshpande VS, Neddleman A, Van der Giessen E. Int J Plast 2008;24:2149.
[20] Balint DS, Deshpande VS, Neddleman A, Van der Giessen E. J Mech Phys Solids 2006;54:2281.
[21] Cleveringa HHM, Van der Giessen E, Needleman A. Int J Plast 1999;15:837.
[22] Nabarro FRN. Adv Phys 1952;1:269.
[23] Law E, Pang SD, Quek ST. Compos Part B – Eng 2011;42:92.
[24] Rintoul MD, Torquato S. J Colloid Interf Sci 1997;186:467.
[25] Segurado J, Llorca J. J Mech Phys Solids 2002;50:2107.
[26] Chawla N, Shen YL. Adv Eng Mater 2001;3:357.
[27] Weibull W. J Appl Mech 1951;18:293.
[28] Bassani JL, Needleman A, Van der Giessen E. Int J Solids Struct 2001;38:833.
[29] Bittencourt E, Needleman A, Gurtin ME, Van der Giessen E. J Mech Phys Solids 2003;51:281.
[30] Xue Z, Huang Y, Li M. Acta Mater 2002;50:149.
[31] Yefimov S, Groma I, Van der Giessen E. J Mech Phys Solids 2004;52:279.